



## Particle in box: A cell for in-situ measurements of porosity and effective diffusion coefficient during thermophysical transformations

Mariern Kacem, Sylvain Salvador, Ange Nzihou, Gilles Flamant

### ► To cite this version:

Mariern Kacem, Sylvain Salvador, Ange Nzihou, Gilles Flamant. Particle in box: A cell for in-situ measurements of porosity and effective diffusion coefficient during thermophysical transformations. Industrial and engineering chemistry research, 2007, 46 (20), p. 6558-6565. 10.1021/ie061370k . hal-01634391

**HAL Id: hal-01634391**

**<https://hal.science/hal-01634391>**

Submitted on 16 Mar 2018

**HAL** is a multi-disciplinary open access archive for the deposit and dissemination of scientific research documents, whether they are published or not. The documents may come from teaching and research institutions in France or abroad, or from public or private research centers.

L'archive ouverte pluridisciplinaire **HAL**, est destinée au dépôt et à la diffusion de documents scientifiques de niveau recherche, publiés ou non, émanant des établissements d'enseignement et de recherche français ou étrangers, des laboratoires publics ou privés.

# Particle in Box: A Cell for in-situ Measurements of Porosity and Effective Diffusion Coefficient during Thermophysical Transformations

Mariem Kacem,<sup>\*,†</sup> Sylvain Salvador,<sup>†,‡</sup> Ange Nzihou,<sup>†,§</sup> and Gilles Flamant<sup>†,||</sup>

UMR 2392 CNRS—Centre de Recherche d'Albi en génie des Procédés des Solides Divisés, de l'Energie et de l'Environnement, Ecole des Mines d'Albi Carmaux, Campus Jarlard, 81013 Albi CT Cedex 09, France, Laboratoire Procédés, Matériaux et Energie Solaire, PROMES-CNRS, 66120 Font-Romeu, France

The aim of this work is to develop an experimental device for the measurement of porous media textural properties during physical or chemical transformation. The method is based on gas tracer experiments. The system investigated consists of a spherical reactor containing a spherical porous media. To avoid surface stresses, there is no contact between the sample and the reactor. We called the cell a particle in box, or "PIB". The porosity of the solid and the gas effective diffusivity were determined using a parametric identification method. The model is based on the perfectly stirred reactor approach. The PIB methodology was first checked at room temperature to determine the solid porosity and the effective diffusion coefficient. Experiments were then performed during transformation of a sample composed of a mixture of hydroxylapatite particles, glycerol, and water. In situ determination of the porosity and diffusivity from room temperature to 573 K (300 °C) was demonstrated.

## 1. Introduction

Heat treatment generates morphology transformations inside porous materials that affect their transport properties. Consequently, qualification of these transformations is a key point for realistic modeling.

The ultimate goal may be defined as finding methods that allow in-situ and on-line measurements of morphology transformation during the heat treatment. But, presently, most work deals with measurements at ambient temperature after sample cooling. Different characterization methods based on gas adsorption or microscopic analyses have been proposed.<sup>1–5</sup> Research is mainly focused on relating structural properties and reactions kinetics.

Realistic information may be given by in-situ characterization of porous media. The first step is the observation of transformations, as proposed by Nzihou and Adhikari.<sup>6–7</sup> They have monitored sintering of hydroxylapatite containing lead oxide using an environmental scanning electron microscope (ESEM). Other researchers use Synchrotron microtomography to study densification of porous media.<sup>8–10</sup> A second step aims at measuring a pertinent property that is strongly affected by the transformations, for example, diffusivity. Wicke and Kallenbach's cell<sup>11</sup> is well-known for diffusivity measurements at room temperature. Shigeno et al. modified this cell to perform diffusivity measurement during hematite reduction at different temperatures.<sup>12,13</sup> These authors have reported good results, but methods remain expensive and difficult to implement. We propose a simpler experimental device using a tracer gas method.

It is possible to use a simple cell with a tracer gas method to characterize a particle in-situ during thermophysical transforma-

tions without change of sample size. On the contrary, if the chemical reaction is accompanied by a change of sample size, it is difficult to measure the properties in-situ, because the contact seals between the sample and the walls cannot be maintained, and consequently, the flow conditions vary. In order to overcome this problem, we propose a reactor which respects two requirements:

- avoiding tight contact between the sample and the wall;
- allowing solid property measurement during experiment.

The properties may be measured during transformation, i.e., at different temperatures, and without handling the sample (in-situ and real-time measurements).

Devices respecting these requirements are proposed in the literature. The annular cell is among these solutions. It is made of a cylindrical tube containing a sample (catalyst) of cylindrical form which is positioned axially and around which a fluid circulates in laminar flow. Mass transfer properties are often studied in this type of reactor. For example, Houzelot and Villiermaux<sup>14</sup> studied radial diffusion in an annular reactor in the presence of a first-order chemical reaction. Ghosh and Upadhyay<sup>15</sup> studied mass transfer in such a reactor for Newtonian and non-Newtonian fluids. Mumallah<sup>16</sup> used this reactor to study the reaction of hydrochloric acid with limestone.

The perfectly stirred reactor (PSR) is another solution. By definition, the main property of a PSR is a uniform fluid concentration in the whole reactor volume. Matter exchange is based here on diffusion without privileging any particular geometric direction. The practical difficulty is to obtain this uniformity. This objective may be achieved by various techniques. Brisk et al.<sup>17</sup> and Tajbl et al.<sup>18</sup> suggested mixing catalyst and gases; the pellets of the catalyst were placed in a basket (metal grid) which turned at high speed around an axis. In other works, mixing is carried out by fluidization of the catalyst.<sup>19</sup>

One of the following techniques may be used to maintain a motionless sample and a well-mixed fluid around it:

- mechanical agitation by a propeller; however, this technology results in disturbances due to the agitator. Ford and Perlmutter<sup>20</sup> studied the catalytic dehydration of alcohol in a reactor in which the catalyst is motionless and the gas is agitated by means of a two-blade engine. The Berty reactor,<sup>21</sup> manu-

\* Corresponding author. Phone: (33)6 62 48 61 56. Fax: (33)3 83 59 55 31. E-mail: myriam.kacem@enstimac.fr. Address: 5 rue Canrobert 54000 Nancy, France.

† UMR 2392 CNRS—Centre de Recherche d'Albi en génie des Procédés des Solides Divisés.

‡ E-mail: sylvain.salvador@enstimac.fr.

§ E-mail: ange.nzihou@enstimac.fr.

|| Laboratoire Procédés, Matériaux et Energie Solaire, PROMES-CNRS.

E-mail: Gilles.Flamant@promes.cnrs.fr.

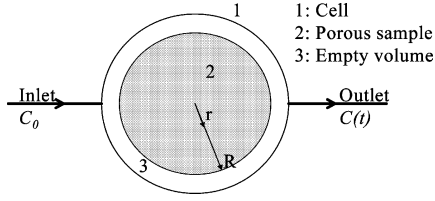


**Figure 1.** Schematic of the particle in box experimental device.

factured using this principle, is marketed and used in various research works.<sup>22</sup>

- turbulences created by jets resulting in intense internal recycling streams.<sup>23–30</sup>

We chose this second method, named in the literature as a “jet-stirred reactor”.

## 2. Identification Model

**2.1. Model.** On the basis of the jet-stirred reactor assumption, gas tracing experiments were performed using purge injection. Then, parametric identification based on a direct model was applied to determine the porosity and diffusion coefficient.

Let us imagine a single spherical particle placed in a well-stirred reactor as illustrated in Figure 1; the cell is called a particle in box or “PIB”. The direct model describes mass transfer in the reactor and inside the sample. For diffusion-controlled gas transport inside the particle (with no molar barycentric velocity), without chemical reaction, the tracer concentration varies according to Fick’s second law in spherical coordinates,

$$\epsilon_p \frac{\partial C_i(t)}{\partial t} = \frac{D_{\text{eff}}}{r^2} \frac{\partial}{\partial r} \left( r^2 \frac{\partial C_i(t)}{\partial r} \right) \quad (1)$$

with  $\epsilon_p$  as the particle porosity,  $D_{\text{eff}}$  as the effective diffusion coefficient, and  $C_i$  as the molar concentration of gas (tracer) in the porous particle.

The boundary conditions are

$$\text{- symmetry at the particle center, } \left. \frac{\partial C_i(t)}{\partial r} \right|_{r=0} = 0 \quad (2)$$

$$\text{- continuity at the particle surface, } C(t)_{\text{particle}} = C_i(t) \quad (3)$$

With regard to the gas in the empty volume of the reactor (neglecting the external resistance located in the particle vicinity), the following relationship is developed:

$$(\text{entering flow}) - (\text{outgoing flow}) =$$

$$(\text{accumulation flow}) + (\text{flow exchanged with the particle})$$

$$QC_0 - QC(t) = V_e \frac{dC(t)}{dt} - \epsilon_p V_p \frac{d\overline{C_i(t)}}{dt} \quad (4)$$

$\overline{C_i(t)}$  represents the average concentration of the fluid in the porous volume of the particle,  $C_0$  is the initial fluid concentration,  $C(t)$  is the fluid concentration,  $V_e$  is the empty volume between the particle and the cell walls, and  $V_p$  is the particle volume. Accounting for eq 1, the mass balance becomes the following:

$$Q(C_0 - C(t)) = V_e \frac{dC(t)}{dt} - SD_{\text{eff}} \left( \frac{\partial C_i(t)}{\partial r} \right)_{r=R} \quad (5)$$

**Table 1.** Porosity at Different Particle Levels Calcined at 5 K·min<sup>−1</sup>

	5 K·min <sup>−1</sup>		
radius	0	$R/2$	$R$
porous volume (cm <sup>3</sup> ·g <sup>−1</sup> )	0.46	0.47	0.47
porosity	0.57	0.57	0.58

A Laplace transform may be used to solve the mass balance equation. The transfer function is thus determined.<sup>22,26,27,31</sup> It is based on a model of mixers in a cascade arrangement with exchange. With respect to this approach, the transfer function  $G(s)$  of a PSR containing a porous solid is

$$\frac{1}{G(s)} = 1 + t_m s + K \frac{t_m s}{1 + t_D s} \quad (6)$$

Where,  $t_m$  represents the gas residence time in the free volume,  $K = \epsilon_p(1 - \omega)/\omega$  is the capacity factor,  $\omega$  is the ratio of free volume between the sample and the cell with respect to the total volume of the cell,  $\omega = (V_c - V_e)/V_c$ ,  $V_c$  is the cell volume, and  $t_D$  is the diffusion time in the particle. The external transfers are often neglected (mainly in the gas phase), and  $t_D$  is thus defined by  $t_D = \epsilon_p \lambda d^2 / D_{\text{eff}}$  with  $\lambda$  being a factor of form ( $\lambda = 3/5$  for a sphere) and  $d$  being the particle equivalent diameter ( $d$  = particle volume/particle surface; for a sphere,  $d = d_p/6$ ). By inversion of the  $G(s)$ , an analytical expression of the response to a purge injection is obtained,

$$\frac{C(t)}{C_0} = X t_1 \exp\left(-\frac{t}{t_1}\right) + Y t_2 \exp\left(-\frac{t}{t_2}\right) \quad (7)$$

$$\text{with } X = \frac{1}{\sqrt{\Delta}} \left( \frac{1}{t_m t_D} + \frac{s_1}{t_m} \right) \text{ and } Y = \frac{-1}{\sqrt{\Delta}} \left( \frac{1}{t_m t_D} + \frac{s_2}{t_m} \right)$$

$\Delta$  is defined by the following:

$$\Delta = \left( \left( \frac{K+1}{t_D} \right) + \frac{1}{t_m} \right)^2 - \frac{4}{t_m t_D}$$

$$s_1 = -\frac{1}{t_1} = -\frac{1}{2} \left( \left( \frac{K+1}{t_D} \right) + \frac{1}{t_m} - \sqrt{\Delta} \right) \text{ and } s_2 = -\frac{1}{t_2} = -\frac{1}{2} \left( \left( \frac{K+1}{t_D} \right) + \frac{1}{t_m} + \sqrt{\Delta} \right)$$

The assumption of sample spherical symmetry and homogeneity was checked using the following tests:

- measurements of sphere diameter at different points around the sphere. A  $\pm 2\%$  error was measured.

- verification of the porosity distribution homogeneity at different positions inside the spherical sample (See Table 1).

The porosity can be determined from an interpretation of the elution curve after the gas transition. The surface method is based on the integration of the surface area below the response curve that makes it possible to calculate the total volume of the gas inside the cell. Since the volume of the sample and the volume of the dead zones are known, the porosity can be calculated as  $\epsilon_p = V_{\text{pore}}/V_{\text{sample}}$ . The dead zone volume can determine by the elution curve of the experimental apparatus with a nonporous medium (two times measurements method).

**2.2. Parametric Identification.** The sensitivities of the direct model response curve to changes in porosity and in effective diffusion coefficient are not correlated. Therefore, the simultaneous identification of a single value for each parameter is possible. The parameter identification method used is based on the Nelder–Mead simplex algorithm. Thus, we defined an

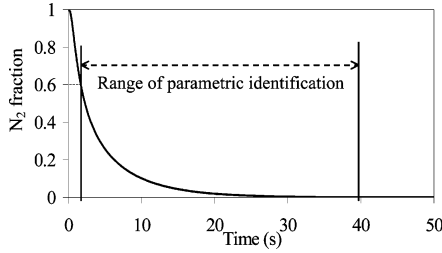


**Figure 2.** Experimental curve range for parametric identification.

objective function (OF) to minimize the differences between the experimental response curve and the model response curve (eq 8). It corresponds to the standard deviation between the two curves.<sup>32</sup> For the first iteration, porosity and  $D_{\text{eff}}$  are initialized with typical values.

$$\text{OF} = \frac{1}{i} \left( \sum_{i=1}^i (y_{\text{th}}(t) - y_{\text{exp}}(t))^2 \right) \quad (8)$$

Where,  $i$  is the number of points of each curve,  $y_{\text{exp}}$  and  $y_{\text{th}}$  are the discrete values of the experimental and theoretical response curves, respectively. They correspond to time evolutions of mass fractions.

If the response curve can be considered as being divided into two parts, the first part corresponds to the gas circulation in an empty volume and the second part corresponds to the gas particle diffusion. It has been established by other authors<sup>22</sup> and observed in this work that the response curve is affected by the textural properties of the sample only in the second part of the curve; the first part is affected mainly by the empty volume of the cell and the ideality of the injection signal. As a consequence, the part of the curve from  $t = 0$  to the time  $t$  when  $C/C_0 = 0.6$  (for an  $\text{N}_2$  transition from 100 to 0%) was not taken into account in the calculation of the OF.

Another point to be considered is the choice for the last point of the response curve that should be taken into account. The part of this curve close to  $C/C_0 = 0$  (long times) is very sensitive to  $\epsilon_p$  and  $D_{\text{eff}}$ . Nevertheless, if a small error in the values of  $C/C_0$  is introduced by the detector and integrated over a long period of time, the OF might be significantly altered. We found that stopping the calculation of the OF at the time when  $C/C_0 = 10^{-3}$  was the best compromise.

Finally, the identification was taken between  $t_{C/C_0}$  corresponding to the fraction  $C/C_0$  in the range 0.6 to  $10^{-3}$  (Figure 2).

**2.3. Taking into Account the Dead Volumes.** The response curve of the PIB presents a time shift due to injection and detection systems and the presence of dead volumes. These volumes are distributed both upstream of the cell in the tracer gas injection system and downstream of the cell in the sampling system. They were taken into account in the present work.

Considering  $\tau_{\text{inj}}$  to be the characteristic time of the injection, two methods are used:

- the direct method, namely, the two times measurements method. This consists in measuring the response signal for the injection system directly connected to the sampling system to determine  $\tau_{\text{inj}}$ . This value is then deduced from  $t_m$ .
- the indirect method. Since the temperature and the pressure of the tracer gas may vary from one experiment to another, The determination of the characteristic time  $\tau_{\text{inj}}$  was performed for each experiment by adjusting its value—together with the values of  $\epsilon_p$  and  $D_{\text{eff}}$ —to minimize the OF. It had previously been checked that the set of values  $\tau_{\text{inj}}$ ,  $\epsilon_p$ , and  $D_{\text{eff}}$  was unique and

that forcing another value for  $\tau_{\text{inj}}$  did not lead to another set for  $\epsilon_p$  and  $D_{\text{eff}}$  values with a better value of the OF.

### 3. Experiments

**3.1. Materials. 3.1.1. Samples for Experiments at Room Temperature.** The samples used for the experiments carried out at room temperature were in 45 mm diameter spheres made of glass ceramic prepared through the procedure described elsewhere.<sup>33</sup> The sample is composed of calcium hydroxylapatite Ca-HAp,  $\text{Ca}_{10}(\text{PO}_4)_6(\text{OH})_2$ , of 40  $\mu\text{m}$  mean size and 7 wt % glass binder composed of oxides ( $\text{SiO}_2$ ,  $\text{Na}_2\text{O}$ ,  $\text{K}_2\text{O}$ ,  $\text{MgO}$ ,  $\text{CaO}$ ,  $\text{P}_2\text{O}_5$ , and  $\text{B}_2\text{O}_3$ ). Two samples were prepared: one without gelatin and one in which 5 wt % of gelatin particles of 500  $\mu\text{m}$  mean size was added. Then, Ca-HAp and the glass binder were mixed in water (40 wt %). The pasty mixture obtained was then shaped in a spherical mold and dried at room temperature for 5 days until the weight remained constant.

The dried agglomerate sphere obtained was calcined to evaporate the gelatin and the remaining water, thus generating the porous sample. The calcination experiments were carried out in a 2 L furnace under flowing air in which the samples were placed in an alumina crucible. The heating program was the following:

- heating rate of 1  $\text{K} \cdot \text{min}^{-1}$  from room temperature to the chosen temperature of 573 K (300 °C), and then, an isotherm plateau of 10 min;
- heating rate of 2  $\text{K} \cdot \text{min}^{-1}$  from 573 (300) to 1373 K (1100 °C) followed by a plateau of 30 min;
- cooling at the same rate.

Heating at 1373 K (1100 °C) leads to the complete sintering of the sample. This ensures that the properties of the prepared sample will remain constant during the experiment in the reactor.

The total porosity of the sample was determined using the mercury porosimeter (Autopore III, 9410 Micromeritics). A porosity of 0.61 for the standard sample (prepared with only Ca-HAp, glass, and water) was obtained. The total porosity of the sample prepared with 5 wt % gelatin was 0.66. The pore volume distribution determined by the mercury porosimeter showed that the evaporation of the gelatin during the calcination step created wider macropores than those created with only water evaporation.

**3.1.2. Sample for in-situ Experiments at Variable Temperature.** For the in-situ measurements of the physicochemical transformations under thermal treatment, a sample composed of Ca-HAp, water, and glycerol was prepared. The purpose of the experiment was to follow the chemical and physical changes occurring during the evaporation of water and during the evaporation of glycerol. So, a sample made of Ca-HAp and 30 wt % of a 25 wt % glycerol solution was molded and dried at room temperature for 5 days, until the weight remained constant. A spherical sample was obtained.

A total porosity of 0.43 was determined for this sample using the mercury porosimeter.

Prior to the investigation of the behavior of the sample in the PIB, the thermal behavior of this sample was characterized using the thermogravimetric analysis-differential scanning calorimetry (TGA-DSC; Netzsch STA 409) analyzer. The scanning rate was 5  $\text{K} \cdot \text{min}^{-1}$  from room temperature to 573 K (300 °C). The results presented in Figure 3 show two distinct peaks. The first one—completed at 373 K (100 °C)—corresponds to the evaporation of water from the sample, while the second peak is attributed to the evaporation of the glycerol, completed at 633 K (360 °C). This allows performance of characterization



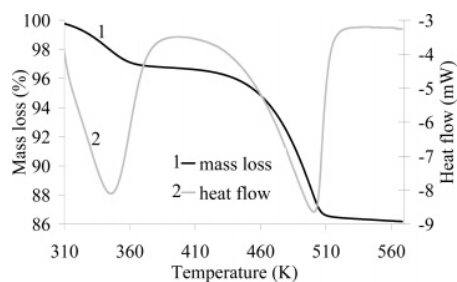


**Figure 3.** TGA-DSC curves for water and glycerol evaporation on the Ca-HAp sample.

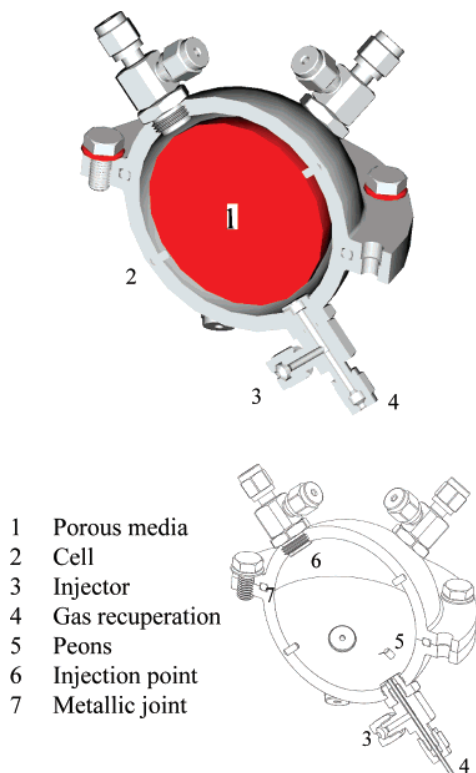
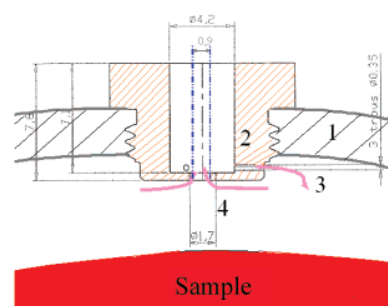


**Figure 4.** PIB cell.

at three times: before evaporations, after water evaporation, and after glycerol evaporation, respectively.

The results presented in Table 1 reveal interesting information on the porosity distribution within the spherical sample heated with our experimental device. So, a solid sampling was made inside the spherical sample volume at different positions: the center of the sample (radius  $r = 0$ ), at  $R/2$ , and at the surface of the sample ( $r = R$ ). The porosity and the pore volume were determined using a mercury porosimeter for each sample. The results show that the porous sample prepared has a uniform pore distribution and thus could be adopted for the experiments aiming to investigate the chemical and physical changes in a homogeneous spherical solid during thermal treatment.

**3.2. Experimental Device.** The new experimental device (PIB) set up to follow the changes during the thermal treatment is made of two stainless steel hemispheres 5 cm i.d. The spherical reactor with one hemisphere removed is shown in Figure 4. The objective was to design a perfectly stirred flow system at steady state. Ideally, pure gas enters the reactor and is instantaneously and perfectly mixed with the gas within the reactor. Simultaneously, products of tracing are withdrawn from the cell volume, and the exiting flow rate is equal to the entering flow rate. The gas enters by six inlet tubes arranged as



1 Cell seal 3 Gas injection (3 jets at 120°)  
2 Injector/recuperate point 4 Gas exit

**Figure 5.** Detail of the inlet/outlet gas point.

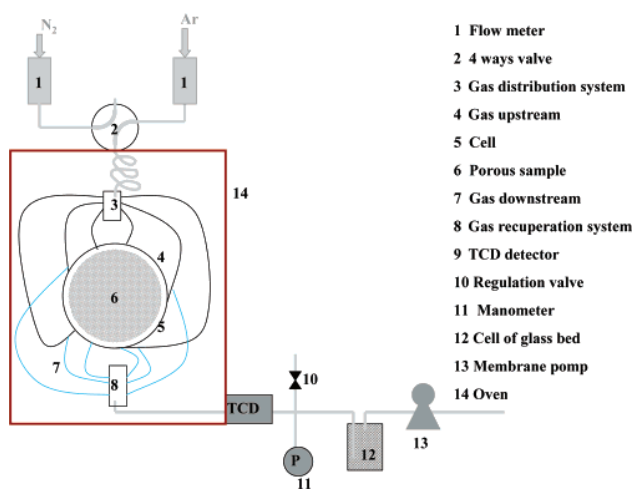


**Figure 6.** Experimental apparatus of the PIB cell.

symmetrically as possible in the reactor. At these points, an inlet/outlet device was made (Figure 5). Each one of them contains three injections holes, 0.35 mm in diameter. The mixture flows as small jets from the holes to the sample and into the surrounding gases. The mixture of gases fills the volume bounded by the inner seal and the inlet tubes and sample. The 18 small inlet mixture jets stir the reactor vigorously to make it homogeneous. The gas mixture exits through six outlet tubes, 1.7 mm in inner diameter (wider than the inlet ones to facilitate the evacuation of the gas from the reactor), placed in the center of the inlet/outlet device (Figure 5). The entire assembly is enclosed in a recuperation system. Upstream of the cell, gases cross the flow controllers and a four-way valve in a 0.9 mm inner diameter tube. At the furnace inlet, the tube has a spiral form and it is connected to a gas distribution system.

The analysis of gases exhausted from the reactor was carried out using a thermal conductivity detector (TCD) gas chromatograph directly connected to the exit reactor by a tube placed in the gas recuperation system. A membrane pump and a valve placed after the chromatograph ensured a constant flow rate in the detector. The reactor was placed inside the chromatographer furnace. Argon and nitrogen were used as scanning gases (Figures 6 and 7).

The TCD calibration curve is established using the two mass flow meters by feeding gas mixtures—with different fractions of the two gases—at a constant total volume flow rate. A calibration curve with a standard deviation  $r^2$  better than 0.998 is typically obtained.

The volume ratio (sample volume/cell volume) is then about 0.72. A preliminary study has demonstrated that the sensitivity

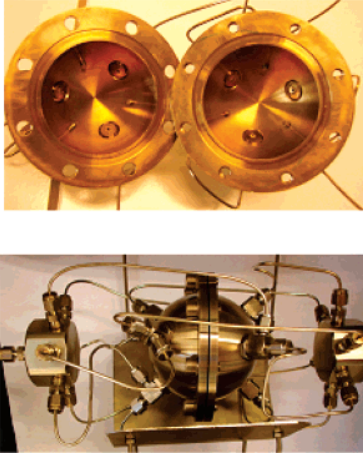


Figure 7. Photos of the PIB cell.

to porosity and to diffusivity is better for high values of the volume ratio. This has been also observed in the work of Ahn,<sup>22</sup> who suggests using a maximal volume ratio to precisely determine diffusivity. Thus, the ratio 0.72 was the maximum value technically feasible in our case.

**3.3. Determination of the Operating Conditions. 3.3.1. Value of the Tracer Gas Flow Rate.** The tracer gas flow rate should be high enough for the cell to behave as a PSR reactor whatever the operating temperature. In order to characterize the mixing in the cell, an experiment was run with a 44.5 mm diameter nonporous metal sphere placed in the cell. In the preliminary sensitivity study, it was demonstrated that porosity and diffusivity determination are better with a low flow rate. The criterion to determine the minimum flow rate was that the experimental number of mixers  $N_{\text{mix}}$  should be in the range  $1 \pm 0.05$ . Indeed for the model under consideration, the number of mixers ( $N_m$ ) is equal to 1. The difference between the ideal case ( $N_m = 1$ ) and a real case may be evaluated by a number of mixers larger than one. Buffham and Gibilaro<sup>34</sup> consider that the number of mixers is not an integer.  $N_{\text{mix}}$  is determined from the characteristic response of a PSR to a purge injection,

$$\frac{C}{C_0} = \exp\left(-\frac{t}{\tau}\right) \quad (9)$$

$$\text{with } \tau = \frac{V_c}{Q}$$

Then,  $\tau$  was calculated. If an experiment is run, an experimental value  $\tau_{\text{exp}}$  can be determined by fitting this model with the experimental response. The number of mixers is then defined by

$$N_{\text{mix}} = \frac{\tau_{\text{exp}}}{\tau} \quad (10)$$

Experiments showed that for a flow rate of  $1.3 \times 10^{-5} \text{ m}^3 \cdot \text{s}^{-1}$  and temperatures of 303 (30), 383 (110), and 573 K (300 °C) the reactor effectively behaves as a PSR. At 303 K (30 °C), this flow rate corresponds to a velocity of  $7.7 \text{ m} \cdot \text{s}^{-1}$  in the 18 injection jets.

It has been observed that the pressure inside the cell changed when the operating temperature was varied. For instance, it increased from 102.3 kPa at room temperature to 104 kPa at 573 K (300 °C). The mass flow rates injected in the experiments

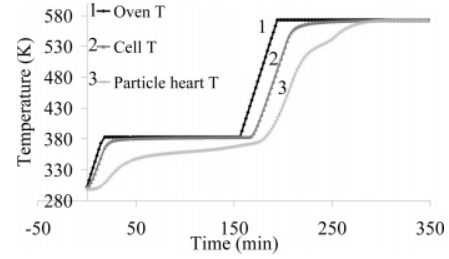


Figure 8. Temperature evolution at different parts in the cell under heat treatment.

through the mass flow meters were calculated taking into account both the actual pressure and the temperature inside the cell.

**3.3.2. Value of the Heating Rate during Experiments under Thermal Treatment.** During the experiment *under thermal treatment*, the sample was heated and the temperature was first stabilized at 383 K (110 °C), and then heated again before finally stabilizing the temperature at 573 K (300 °C). The heating-rate value is a key parameter for the experiments. Indeed, if the sample is heated at too high a heating rate, the temperature evolution at the center of the sample will be very different from that at the surface. As a consequence, the sample may undergo strong mechanical constraints and the textural transformations may not be uniform inside it. On the other hand, heating rates that were too small would require very long experiments.

In order to characterize the heating rate, an experiment was run during which a thermocouple was placed at the heart of a sample and another thermocouple was placed in the empty space inside the cell. The sample was a Ca-HAp sphere; the two endothermic reactions of water evaporation and glycerol evaporation occurred.

Figure 8 plots the temperature versus time evolution of the two thermocouples together with the furnace temperature in the case of a heating rate of  $5 \text{ K} \cdot \text{min}^{-1}$ . The curves indicate that temperature difference between the heart of the sample and the surrounding gas remains less than 100 K even during the heating phase. We estimate that this difference remains acceptable. In the range 220 to 250 min, one can observe a small decrease in the slope of the sample temperature, which is due to the endothermic evaporation of glycerol. After 100 min following a heating phase, the sample was almost isothermal; the characterization experiments were run after this stabilization period.

**3.3.3. Effect of a Change of the Sample Diameter.** The physical transformations undergone by the sample may induce a change in its diameter. If an error is introduced in the sample diameter during the parameter estimation procedure, the derived characteristic will be affected. In order to evaluate this quantitatively, the error on the fitted parameters due to 1% (0.5 mm) error on the sample diameter was calculated. It was found that the error for the sample porosity was less than 0.01% and that the error on the effective diffusivity was 5.6%. Consequently, an uncertainty in the sample diameter of 2% remains acceptable.

At this stage, the PIB experiment was not associated with a sample diameter measurement device. Prior to the experiment under thermal treatment, it was necessary to determine the change in diameter of the sample during heating up to 573 K (300 °C). Thermal mechanical analysis (TMA; Setaram Setsys 16/20) was used. Figure 9 illustrates the TMA curves for a cylindrical sample 3.98 mm in diameter and 13.2 mm long submitted to the following thermal treatment: heating from 303

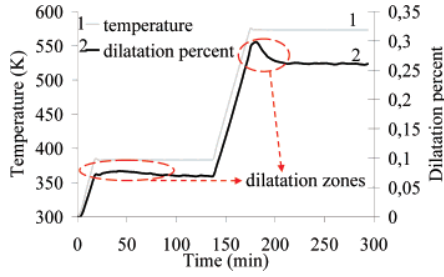


**Figure 9.** TMA of the Ca-HAP sample with 30 wt % of a solution of 25 wt % glycerol dried at room temperature.

**Table 2. Results of Parametric Identification for the Two Different Porous Samples with and without Gelatin**

		sample w/o gelatin	sample 5% gelatin
$\epsilon_p$	mercury porosimeter	$0.61 \pm 1.8\%$	$0.66 \pm 1.9\%$
	surface method	0.59	0.64
	parametric identification	0.58	0.63
$D_{eff}$ ( $m^2 \cdot s^{-1}$ )	parametric identification	$6.41 \times 10^{-6} \pm 11\%$	$7.83 \times 10^{-6} \pm 12\%$

(30) to 383 K (110 °C) at  $5 \text{ K} \cdot \text{min}^{-1}$  and holding for 2 h, followed by heating from 383 to 573 K (300 °C) at  $5 \text{ K} \cdot \text{min}^{-1}$  and holding for 2 h. The curve shows two dilatation zones during the heating periods, both followed by zones where the sample size is stable. The total dilatation of the sample is 0.26%, which is satisfactory for the experiments in the PIB cell without radius particle change.

**3.3.4. Estimation of the Total Error in the Determination of the Sample Properties.** The uncertainty on the values for the sample porosity and the sample effective diffusivity is difficult to determine exactly; it is estimated as follows. It is assumed that the main uncertainties are introduced through the tracer gas flow rate,  $\pm 1\%$ ; the sample diameter,  $\pm 0.4\%$ ; the diameter of the cell,  $\pm 0.2\%$ ; and the analysis of the tracer gas (determined by reproducibility method),  $\pm 0.01\%$ .

Finally, it was found (from a number of simulations combining the errors on all parameters and trying to maximize the total error) that the PIB cell method could determine the parameters with a minimum error of  $\pm 1.9\%$  for sample porosity and  $\pm 7.2\%$  for the diffusivity.

## 4. Results and Discussion

**4.1. Experiments at Room Temperature.** The first experiments were run at room temperature, using two biomaterials. The first one was prepared without gelatin, while 5 wt % gelatin was used for the second one. The experiments were repeated 3 times for each sample; the averaged values obtained are reported in Table 2. As also indicated in the table, the scatters between the values during repeatability tests were less than  $\pm 2\%$  for porosity and less than  $\pm 12\%$  for diffusivity. The values obtained for  $\epsilon_p$  can be compared with the values obtained from other methods, including the mercury porosimeter and surface methods (Table 2). For the two biomaterials, the difference between the measured porosity using the PIB and the values from the two reference methods is 2% only; this result is very satisfactory. One can also note that, for a given measurement technique, the sample prepared with 5% gelatin—which is removed during the preparation process—exhibits 5% more porosity than the sample prepared without gelatin.

A good agreement is found for the value of porosity determined by various methods. The values of  $D_{eff}$  are close,

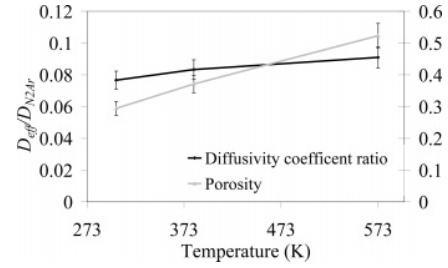


**Figure 10.** Porosity and  $D_{eff}/D_{N2Ar}$  evolution during the thermal process as found from PIB.

both with and without gelatin. The presence of gelatin influences pore distribution and porosity but does not significantly influence  $D_{eff}$ .

**4.2. Measurement Reproducibility.** To evaluate measurement error, different tracer experiments were done for the same sample and in the same experiment conditions. A comparison between response signals shows a good repeatability of the signal, the mean deviation for all points being about  $2.8 \times 10^{-3}$ .

**4.3. Experiments under Thermal Treatment.** The next step in the evaluation of the PIB was to determine  $\epsilon$  and  $D_{eff}$  for a sample that undergoes textural changes between two characterizations. One characterization was realized on the initial sample at room temperature, while two were operated *under temperature*, at 383 (110) and 573 K (300 °C).

The sample was therefore placed in the cell and characterized, then heated to 383 K (110 °C) at  $5 \text{ K} \cdot \text{min}^{-1}$ , and maintained at this temperature for 3 h and characterized. It was finally heated to 573 K (300 °C) (again at  $5 \text{ K} \cdot \text{min}^{-1}$ ) and maintained for 3 h at this temperature before the third and final characterization. All results are reported in Figure 10. In order to eliminate the effect of temperature on  $D_{eff}$ , the results for diffusivity are expressed through the ratio  $D_{eff}/D_{N2Ar}$ .

The sample porosity is found initially at 0.30 and increases to 0.36 after removal of the water and to 0.52 after removal of the glycerol. Mercury porosimetry requires submitting the sample to vacuum, which induces the removal of water and glycerol: it could not be used for the initial sample and the sample after removal of the water. The porosity of the final sample was measured at 0.55 which is very close to the value of 0.52 determined at 573 K (300 °C) using the PIB. Since the TMA has shown that the sample size does not change significantly along the heating process, this agreement can be taken as a validation.

It can be noted that the mass loss during water removal measured from the TG experiment is 3%, and the increase in porosity due to this transformation is  $0.36 - 0.3 = 0.06$ . As far as glycerol removal is concerned, the mass loss is 11% while the increase in porosity is  $0.53 - 0.36 = 0.17$ .

The total porosity of the initial sample was calculated at 0.4 from the measurement of its true density measured using helium pycnometry (Micrometrics, Accupyc 1330); the value of the porosity derived from the PIB is 0.30. The difference between the two values can be attributed to closed porosity, which is not taken into account by the PIB cell. After the two evaporations, the true density of the sample measured is equivalent to a porosity of 0.55. This value is in good agreement with the previously determined ones.

The ratio  $D_{eff}/D_{N2Ar}$  increases from 0.077 for the initial sample to 0.083 for the sample after the removal of the water and to 0.091 after the removal of glycerol. Unfortunately, no reference technique was available to compare with these values.

Diffusivity depends on the porosity and tortuosity factor of porous media. The morphological model of a cylindrical



capillary gives  $D_{\text{eff}} = \epsilon_p / \tau D_{\text{N}_2\text{Ar}}$ . The water and glycerol evaporation increase the porosity. The tortuosity factor evolution is more complex to explain because liquid can evaporate through the shortest path resulting in a decrease in the tortuosity factor and liquid connection with the solid can close pores inside the material. When evaporation occurs, tortuous paths can be created.

## 5. Conclusion

A new cell that enables the simultaneous determination of porosity and of effective diffusivity of a single porous sphere (45 mm i.d.) within less than 1 min has been successfully developed. The sphere sample is neither in contact with the cell walls that contains it nor in contact with any tightness system; this allows small changes in the diameter of the sample to occur. The measurements can be taken under temperature, without cooling the sample prior to characterization.

By injecting the tracer gas through 18 jets, the conditions of PSR in the empty volume of the cell were obtained for a tracer gas flow rate of  $1.3 \times 10^{-5} \text{ m}^3 \cdot \text{s}^{-1}$ .

The first tests at room temperature indicated that the values for porosity determined from the PIB were in very good agreement with two reference techniques.

The tests performed under thermal treatment proved that measurements at temperatures up to 573 K were possible. The scattering in the values determined when the characterization experiment was repeated several times did not exceed  $\pm 2\%$  porosity.

The values of the diffusivity coefficient found in this work are in agreement with known values for gases in porous materials. Nevertheless, the error for diffusivity measurement is more important than for porosity measurement. It is known that diffusivity values found using different measurement techniques are not equal for the same system.<sup>35</sup> Thus, the error found in this work is acceptable.

The parameter identification procedure is based on a quite direct model that describes the experiment. Nevertheless, it requires a number of precautions. The dead volumes in the tracer gas injection and sampling devices have to be taken into account. The objective function that compares the experimental response to the model-predicted one should be calculated on a limited period of time during the experiment.

The work shows that the diameter of the sample should be known with an accuracy of  $\pm 0.5 \text{ mm}$  for the measurements to be accurate. Experiments were run with samples whose diameter did not change significantly along the heating process. In the case where the diameter might change more significantly, the PIB should be combined with an online diameter measurement system.

Experiments were carried out during temperature plateau and after waiting for the end of the transformation. Thus, one can expect that the PIB will make it possible to follow the textural transformation continuously along the heating process in the case of slow transformations.

## Literature Cited

- (1) Vix-Guterl, C.; Shah, S.; Dentzer, J.; Ehrburger, P.; Manocha, L. M.; Patel, M.; Manocha, S. Carbon/carbon composites with heat-treated pitches II. Development of porosity in composites. *Carbon* **2000**, *38*, 673.
- (2) Liming, L.; Sahajwalla, V.; Harris, D.; Coal Char Reactivity and Structural Evolution during Combustion-Factors Influencing Blast Furnace Pulverized Coal Injection Operation. *Metall. Mater. Trans. B* **2001**, *32B*, 811.
- (3) Zhang, L. H.; Calo, J. M. Thermal desorption methods for porosity characterization of carbons and chars. *Colloids Surf. A* **2001**, *187*, 207.

- (4) Feng, B.; Bhatia, S. K.; Barry, J. C. Structural ordering of coal char during heat treatment and its impact on reactivity. *Carbon* **2002**, *40*, 481.
- (5) Park, K.; Seo, D. J. Gas sensing characteristics of BaTiO<sub>3</sub>-based ceramics. *Mater. Chem. Phys.* **2004**, *85*, 47.
- (6) Nzihou, A.; Adhikari, B. Effect of oxides and nitrates of lead on the sintering and densification of hydroxyapatite adsorbents. *Ind. Eng. Chem. Res.* **2004**, *43* (13), 3325.
- (7) Nzihou, A.; Adhikari, B.; Pfeiffer, R. Effect of metal chlorides on the sintering and densification of hydroxyapatite adsorbents. *Ind. Eng. Chem. Res.* **2005**, *44*, 1787.
- (8) Gendron D. Etude numérique et expérimentale du frittage à l'échelle du grain. Ph.D. thesis, University of Bordeaux I, France, 2001.
- (9) Lame, O.; Bellet, D.; Di Michiel, M.; Bouvard, D. Etude de l'évolution microstructurale de poudres métalliques en cours de frittage par microtomographie. *Rev. Metall.* **2001**, *SF2M* 2001, 185.
- (10) Lame, O.; Bellet, D.; Di Michiel, M.; Bouvard, D. *Analyse du frittage de poudres métalliques par microtomographie synchrotron in situ*; Colloque De la poudre au matériau massif, Ecole des Mines d'Albi-Carmaux, 2003, 189.
- (11) Wicke, E.; Kallenbach, R. Die Oberflächen diffusion von Kohlendioxid in aktiven Kohlen. *Kolloide Z.* **1941**, *2*, 135.
- (12) Shigeno, Y.; Sakakibara, T.; Omori, Y. High Temperature Measurement of the Effective Diffusivity through Coke and Graphite by the Wicke-Kallenbach method. *Trans. Iron Steel Inst. Jpn.* **1988**, *28*, 697.
- (13) Shigeno, Y.; Sakakibara, T.; Omori, Y. In situ measurement of effective gas diffusivity through hematite pellets during stepwise reductions. *Metall. Trans. B* **1990**, *21B*, 677.
- (14) Houzelot, J. L.; Villiermaux, J. Mass transfer in annular cylindrical reactors in laminar flow. *Chem. Eng. Sci.* **1977**, *32*, 1465.
- (15) Ghoshand U. K.; Upadhyay, S. N. Mass transfer to Newtonian and non-newtonian fluids in short annuli. *AIChE J* **1985**, *31*, 101721.
- (16) Mumallah, N. A. Hydrochloric acid diffusion coefficients at acid-fracturing conditions. *J. Pet. Sci. Eng.* **1996**, 15361.
- (17) Brisk, M. L.; Day, B. E.; Jones, M.; Warren, J. B.; Development of a stirred gas-solid reactor for the measurement of catalyst kinetics. *Trans. Inst. Chem. Eng.* **1968**, *46a*, 3.
- (18) Tjabl, D. J.; Simons, J. B.; Carberry, J. J. Heterogeneous catalysis in a continuous stirred tank reactor *Ind. Eng. Chem. Fundam.* **1966**, *5*, 171.
- (19) Anderson, R. B. *Experimental methods in catalytic research*; Academic Press: New York and London, 1968.
- (20) Ford, F. E.; Perlmutter, D. D. The kinetics of the brass-catalysed dehydrogenation of sec-butyl alcohol. *Chem. Eng. Sci.* **1964**, *19* (6), 371.
- (21) Berty, J. M. Reactor for vapor-phase catalytic studies. *Chem. Eng. Prog.* **1947**, *70*, 78.
- (22) Ahn, B. J. Etude des caractéristiques diffusionnelles de transfert de matière dans un réacteur catalytique à lit fixe d'oxydation ménagée. Ph.D. thesis, Technology University of Compiègne, France, 1980.
- (23) Longwell, J. P.; Weiss, M. A. High temperature reaction rates in hydrocarbon combustion. *Ind. Eng. Chem.* **1955**, *47* (8), 1634.
- (24) Bush, S. F. The design and operation of single-phase jet-stirred reactors for chemical kinetic studies. *Trans. Inst. Chem. Eng.* **1969**, *47*, 59.
- (25) Matras, D.; Villiermaux, J. Un réacteur continu parfaitement agité par jets gazeux pour l'étude cinétique de réactions chimiques rapides. *Chem. Eng. Sci.* **1973**, *28*, 129.
- (26) Matras, D. Conception et essais d'un réacteur auto agité pour l'étude cinétique de réactions chimiques rapides en phase gazeuse. Ph.D. thesis, University of Nancy I, France, 1973; p 225.
- (27) Villiermaux, J.; Matras, D. Une nouvelle formulation dynamique des interactions fluide solide- Application à des mesures de diffusivités intraparticulaires et de constantes d'équilibre d'adsorption. *Can. J. Chem. Eng.* **1973**, *51*, 636.
- (28) David, R.; Houzelot, J. L.; Villiermaux, J. A novel and simple jet-stirred reactor for homogeneous and heterogeneous reactions with short residence times. *Chem. Eng. Sci.* **1979**, *34*, 867.
- (29) Dagaut, P.; Reuillon, M.; Cathonnet, M. Experimental study of the oxidation of n-heptane in a jet stirred reactor from low to high temperature and pressures up to 40 Atm. *Combust. Flame* **1995**, *101*, 132.
- (30) Côme, G. M.; Li, Y.; Barbe, P.; Gueritey, N.; Marquaire, P. M.; Baronnet, F. Competition between gas and surface reactions in the oxidative coupling of methane 2. Isothermal experiments in a catalytic jet-stirred gas phase reactor. *Catal. Today* **1996**, *30*, 215.
- (31) Villiermaux, J. Theory of linear chromatography. In *Percolation Processes: Theory and Application*; Rodrigues, A. E.; Tondeur, D., Eds.; Sijthoff: Amsterdam, 1981.
- (32) Villiermaux, J.; Antoine, B. Construction et ajustement des modèles mathématiques: une science ou un art? *Bull. B.R.G.M. (deuxième série)* **1978**, *4* (section III), 627.



(33) Zahraoui, C. Greffage de biomolécules sur un nouveau biomatériau à base d'hydroxylapatite-application aux implants osseux. Ph.D. Thesis, University of Paul Sabatier, Toulouse, 1999.

(34) Buffham, B. A.; Gibilaro, L. G. A generalization of the tanks-in-series mixing model. *AIChE J.* **1968**, *1* (14), 805.

(35) Authelin, J. R. Etude du transport de matière dans les catalyseurs à base de zéolite par la méthode chromatographique. Cas d'un traceur inerte

en présence et en l'absence de réaction chimique. Ph.D. Thesis, Institut National Polytechnique de Lorraine, France, 1988.